Studies in Conservation

ISSN: (Print) (Online) Journal homepage: www.tandfonline.com/journals/ysic20

Green Alternatives for Archaeological Iron Stabilization

Patrycja Petrasz, Sami Zhioua, Sarah James, Saskia Bindschedler, Pilar Junier & Edith Joseph

To cite this article: Patrycja Petrasz, Sami Zhioua, Sarah James, Saskia Bindschedler, Pilar Junier & Edith Joseph (2024) Green Alternatives for Archaeological Iron Stabilization, Studies in Conservation, 69:sup1, 270-280, DOI: 10.1080/00393630.2024.2336880

To link to this article: https://doi.org/10.1080/00393630.2024.2336880

Published online: 13 Jun 2024.

STUDIES IN CONSERVATION
2024, VOL. 69, NO. S1, S270–S280
https://doi.org/10.1080/00393630.2024.2336880

ORIGINAL RESEARCH OR TREATMENT PAPER

OPEN ACCESS Check for updates

Green Alternatives for Archaeological Iron Stabilization

Alternativas Verdes para la Estabilización del Hierro Arqueológico

Patrycja Petrasz[1,2], Sami Zhioua[2], Sarah James[3], Saskia Bindschedler[2], Pilar Junier[2] and Edith Joseph[1]

[1]Haute Ecole Arc Conservation Restauration, University of Applied Sciences and Arts HES-SO, Neuchâtel, Switzerland; [2]Laboratory of Microbiology, Institute of Biology, University of Neuchâtel, Neuchâtel, Switzerland; [3]Laboratory of Technologies for Heritage Materials (LATHEMA), University of Neuchâtel, Neuchâtel, Switzerland

ABSTRACT

One of the most challenging types of artifact occurring within museum collections is unstable chloride-contaminated archaeological iron. A high chloride concentration causes cracking, flaking and leads to full mineralization, in effect making objects fragile. Consequently, removal of chloride ions plays a key role in stabilization treatment, while preserving the integrity of the corroded iron object. Despite the variety of stabilization methods, all have significant disadvantages, including a lack of sustainability. Within the framework of the Horizon Europe project GoGreen the potential of microbial biosorption to stabilize archaeological iron artefacts is being investigated. Dry biomass of the fungi *Meyerozyma* sp. and *Saccharomyces cerevisiae* was studied to remove chloride ions. Preliminary tests were carried out on artificially-aged steel samples. To assess the activities of the microorganisms' functional groups and biosorption capabilities as a potential green stabilization treatment, analytical techniques including FTIR, Raman spectroscopy, and SEM-EDX were used. The results demonstrate two promising paths for the development of green stabilization treatments based on fungal biomass: passive adsorption into the cell wall and conversion of reactive corrosion products into more stable compounds. The use of microbial biomass opens up promising perspectives for the development of more sustainable solutions in archaeological iron stabilization, while avoiding the generation of toxic waste in our environment.

Uno de los tipos de artefactos más desafiantes que se encuentran en las colecciones de los museos es el hierro arqueológico inestable contaminado con cloruro. Una alta concentración de cloruro provoca grietas, descamación y conduce a una mineralización completa, lo que de hecho vuelve los objetos frágiles. En consecuencia, la eliminación de iones cloruro juega un papel clave en el tratamiento de estabilización, preservando al mismo tiempo la integridad del objeto de hierro corroído. A pesar de la variedad de métodos de estabilización, todos tienen desventajas importantes, incluida la falta de sostenibilidad. En el marco del proyecto GoGreen de Horizonte Europa, se está investigando el potencial de la biosorción microbiana para estabilizar artefactos arqueológicos de hierro. Biomasa seca de los hongos *Meyerozyma* sp. y *Saccharomyces cerevisiae* fue utilizada para eliminar iones cloruro. Se llevaron a cabo pruebas preliminares con muestras de acero envejecidas artificialmente. Para evaluar las actividades de los grupos funcionales de los microorganismos y las capacidades de biosorción como posible tratamiento de estabilización verde, se utilizaron técnicas analíticas que incluyen FTIR, espectroscopía Raman y SEM-EDX. Los resultados demuestran dos caminos prometedores para el desarrollo de tratamientos de estabilización ecológicos basados en biomasa fúngica: la adsorción pasiva en la pared celular y la conversión de productos reactivos de corrosión en compuestos más estables. El uso de biomasa microbiana abre perspectivas. prometedoras para el desarrollo de soluciones más sostenibles en la estabilización del hierro arqueológico. evitando al mismo tiempo la generación de residuos tóxicos en nuestro entorno.

ARTICLE HISTORY
Received October 2023
Accepted March 2024

KEYWORDS
Green chemistry; chlorides; archaeological iron; micro-organisms; bio-based stabilization

Química verde; cloruros; hierro arqueológico; micro organismos; estabilización de base biológica

Introduction

Archeological iron artifacts undergo complex corrosion phenomena (Simon et al. 2019) and their structure may vary depending on the burial environment: terrestrial or marine. One of the major causes of iron artifacts' instability is contamination with chlorides (Watkinson 2010) which are the main corrosion accelerator (Rimmer, Watkinson, and Wang 2012). A high chloride concentration causes cracking, flaking and leads to full mineralization, in effect making the

CONTACT Patrycja Petrasz patrycja.petrasz@he-arc.ch Haute Ecole Arc Conservation Restauration, University of Applied Sciences and Arts HES-SO, Neuchâtel 2000, Switzerland; Laboratory of Microbiology, Institute of Biology, University of Neuchâtel, Neuchâtel 2000, Switzerland

objects fragile. Consequently, removal of chloride ions plays a key role in stabilization treatment, while preserving the integrity of the corroded iron object (Drews et al. 2013). Despite evidence that chloride ions may be found in any type of archeological iron artifacts, this article focuses exclusively on iron artifacts recovered from burial environments since their corrosion structure is well studied and better understood.

During burial iron corrodes by an electrochemical process (Selwyn 2004) in which chloride ions are attracted by Fe^{2+} at anodic sites on the metal surface (Watkinson 2010). As a result of ongoing iron corrosion during burial, acidic iron(II) chloride is produced (Turgoose 1993). Recovered, iron artifacts containing acidic iron(II) chloride while exposed to lower relative humidity (RH) and higher oxygen will develop further corrosion, which causes cracking and structural damage (Comensoli et al. 2017). Additionally, in favorable conditions such as the presence of high chloride concentration at low pH the formation of unstable chloride-containing corrosion products such as akaganeite and iron(III) oxyhydroxides is induced (Reguer et al. 2009; Selwyn 2004).

Stabilization of archaeological iron is therefore an essential step in the conservation treatment to prevent the development of further corrosion. In current practice, the primary emphasis is on removing chlorides from artifacts by dechlorination methods. Among the most common and effective treatments are sodium hydroxide and sodium sulphite baths (Kergourlay et al. 2018). During immersion the reduction of corrosion compounds occurs allowing the passive diffusion of soluble chloride ions (Comensoli et al. 2017). Despite the many advantages of this technique, there are also drawbacks regarding efficiency, waste neutralization, human health concerns (Comensoli et al. 2017), and in some cases, occurrence of post-treatment corrosion.

In the past two decades global interest in ethical environmental practices in the cultural heritage field has arisen, following the United Nations climate change policies (Kampasakali et al. 2021). Among the most important points presented in these policies is the need for improvement regarding health and safety, environmental impact, carbon footprint of the products as well as waste management. In certain conservation specializations, a first step has already been made towards green conservation by introducing green materials such as biodegradable solvents, bio-based chelates, bio-originated gels, enzymes and microorganisms. Nevertheless, none of these materials can be successfully applied for archeological iron stabilization. Therefore, considering the drawbacks of currently-used archeological iron stabilization methods mentioned above, green conservation faces the challenge of creating effective iron stabilization treatments, while meeting the latest ethical criteria concerning sustainability.

Research in the field of biotechnology opens up a new opportunity for iron dechlorination using the physicochemical abilities of microorganisms. Biosorption, which utilizes passive adsorption of non-living or living biomass to bind ions to the cell's surface, is one of the possible pathways. This approach has been extensively studied in many domains with successful results in removal efficiency of various pollutants such as heavy metals, phenols, fluoride and dyes (Michalak, Chojnacka, and Witek-Krowiak 2013). Biosorption technologies present- good prospects as they are inexpensive, time efficient, and eco-friendly. Despite all the advantages, it is important to mention that biosorption is very complex and it is affected by many factors: pH, contact time, competition with other pollutants, large surface area, high porosity, type and amount of functional groups as well as the cell structure. Therefore, it is important to consider these criteria in the choice of fungal strain and to determine the conditions that will allow interaction between biomass and pollutant.

This study investigates the possibility of using dry biomass from the fungi *Meyerozyma* sp. and *Saccharomyces cerevisiae* as an alternative sustainable treatment for iron stabilization by biosorption. In the first stage the pH and electrode potential of artificially-aged iron and dry biomass were analyzed to predict favorable conditions for biosorption of chloride ions without interfering with the structure of the iron artifacts. Afterwards, biosorption experiments were conducted to investigate passive adsorption in the selected fungi and the processes that influence efficiency. Due to the preliminary character of these experiments, only artificially-aged iron samples were utilized.

Material and methods

Artificially-aged iron samples

Description of samples

The test samples used in the study were artificially-aged steel coupons, size 10 × 10 × 1 mm. Simulation of archeological iron corrosion was based on an aging protocol presented by Glotch and Kraft (2008) that includes a pretreatment step with 0.2M $FeCl_3$, followed by wet/dry cycles in a climatic chamber (wet – 24 h at 30°C with 80–100% RH and dry – 24 h at 30°C with 50–60%RH). To allow akageneite synthesis, NaOH spray was introduced during the first wet cycle phase.

Elemental composition

To determine the elemental composition of the test samples before and after the experiment, X-ray fluorescence spectroscopy was performed using a Niton XL3t GOLDD+ XRF analyzer coupled with helium flow and using a light range filter (0–12 keV) to permit the

detection of light elements, including chlorine. Acquisition time was 3 min.

Molecular characterization

The chemical composition was analyzed with a Renishaw Virsa Raman system. Spot measurements were conducted at room temperature with a 785 nm diode excitation laser, 50× objective and a spectral resolution of ~2 cm^{-1}. In order to avoid excessive heating and potential transformation of iron compounds, the laser power was set to 2–5 mW (Azoulay et al. 2013). Raman spectra were recorded with an acquisition time between 2 and 10 s with 5–20 accumulations. The interpretation of the Raman spectra was performed by comparison with published scientific data and commercial spectra libraries (Vietti et al. 2022).

Preparation of dry biomass

Fungi strains

The selection of yeast strains was based on literature studies. The choice of a strain of *Meyerozyma* spp. was dictated by a fast growth rate (between 2 and 7 days), a large surface area, and high tolerance towards a saline environment that gives promising prospects for chloride ion removal (Amorim et al. 2018; Navarro-Arias et al. 2019). *Saccharomyces cerevisiae* is characterized by a large surface area (Ivanova et al. 2020), porous cell wall (Hu et al. 2019) as well as the ability to under go meiosis (Paulissen et al. 2020) that makes it also an attractive candidate for biosorption studies. Another advantage of *S. cerevisiae* is that it can be obtained as a waste product from beer production, making it easily accessible and inexpensive.

Preparation

Pre-cultures of *Meyerozyma* sp. and *S. cerevisiae* beer waste were provided by the laboratory of microbiology of Neuchatel University. To produce sufficient amounts of dry biomass, *Meyerozyma* sp. was inoculated in liquid malt broth (15 g malt per liter of deionized water) and cultured for 10 days. The resultant yeast culture was autoclaved and washed twice with deionized water. Following 60 min storage at − 80°C, biomass was then transferred to a freeze-dryer for 32 h. The frozen biomass was then ground using a pestle and mortar and sieved to a fine powder with particle size of 125 µm. The described protocol was applied to both *Meyerozyma* sp. and *S. cerevisiae* beer waste biomass.

Strains characterization

The cell wall surface morphology was examined before and after the experiment using scanning electron microscopy (SEM) coupled with energy-dispersive X-ray spectroscopy (EDS). Biological samples were gold-coated prior to observations. Working conditions were 20 kV electron acceleration voltage and a working distance of 5–7 mm.

To identify the chemical functional groups present in the cell wall, and their role in the biosorption process, Fourier transform infrared spectroscopy (FTIR, using a Thermo Fisher Scientific Nicolet iN10 microscope) was employed in attenuated total reflection mode (using a germanium ATR crystal). The infrared spectra were collected in the range 4000–650 cm^{-1} with 16 scans and a spectral resolution of 4 cm^{-1}. Spectral interpretation was focused on three regions: 2700–3300 cm^{-1} for fatty acids, 1500–1800 cm^{-1} for proteins and peptides, and 600–900 cm^{-1}, as fingerprint regions for microorganisms (Lasch and Naumann 2000).

Determination of pH of point of zero charge (pH_{PZC})

The pH_{PZC} of *Meyerozyma* sp. and *S. cerevisiae* was determined on dry biomass by the salt addition technique (Al-Maliky, Gzar, and Al-Azawy 2021). In a series of 50 ml Sovirel bottles, 25 ml of 0.1M NaCl solution was added and adjusted to pHs of 2, 3, 4, 5, 6, 7, 8, 9, 10, 11, 12 by the addition of few drops of 0.001M NaOH and/or 0.001M HCl. Then 0.05 g of dry biomass was added to each of the pH-adjusted solutions and agitated at 120 rpm for 24 h. Afterwards, the final pH was measured with a digital pH meter. The pH_{pzc} was obtained by plotting ΔpH, the difference between the initial pH of the adjusted NaCl solution (pH_i) and the final pH measured 24 h after the addition of the dry biomass (pH_f), *versus* the initial pH. The pH_{pzc} is the point at which ΔpH = 0.

Biosorption experiment

Tests on artificially-aged iron samples were carried out by immersion in deionized water with dry biomass. In preliminary tests, the dissolution rate of released chloride into water was measured to estimate when the biomass should be introduced. Adsorption capacity and factors that influence adsorption rate were observed by varying the contact time between 15, 30, 45, 60, 90, 120 and 150 min. The bottles were agitated at 120 rpm. For biosorption studies, artificially-aged iron samples were placed in 50 ml Sovirel bottles and 40 ml of deionized water adjusted to pH7 was added. Afterwards, the biomass was collected, filtered and dried in a freeze dryer for 12 h to perform SEM and FTIR analyses. To ensure the reliability of the collected data all tests were run in triplicates.

The efficiency of chloride adsorption was calculated according to following equation:

$$\text{Biosorption efficiency } \% = \frac{C_o - C_e}{C_o} \times 100$$

where C_o is the initial concentration in solution and C_e

is the equilibrium concentration of chlorides released after immersion of the artificially-aged iron samples.

Chloride quantification

The concentration of chloride ions released into the solution was measured using a Hach DR3900 spectrophotometer with LCK311 (mercuric thiocyanate) reagent. Iron concentration was determined by ferrozine assay (Stookey 1970) with a Shimadzu UV-1601 spectrophotometer.

Results

Determination of optimal conditions for the biosorption experiment

pH and Pourbaix diagram

The Fe-H_2O-Cl^- Pourbaix diagram was analyzed to find the optimal conditions of pH and Eh to perform the biosorption experiments. The aim of this analysis was to identify parameters that promote the extraction of harmful ions (Cl^-) without interfering with iron stability. According to the values observed on the diagram, the region between pH 6–8 and Eh −0.65 to −0.22 V was determined to be the most promising area (Figure 1(a)).-(a)). These values were compared with the values of pH of point of zero charge obtained from both fungal biomasses. This allowed us to find pH values that would be in the favorable region for interactions with soluble Cl^- presented in the diagram. From the Pourbaix diagram and the results obtained for both fungi, pH 7 was chosen for the biosorption experiments (Figure 1 (b)) and (c).

Contact time

The effect of *S. cerevisiae* contact time on chloride and iron ions biosorption was investigated for 150 min. After this period a shift in the solution pH level was noticed, with the initially measured pH of 7 dropping to 4.4. Processes of adsorption and desorption were observed in the 150-minute experiment. The concentration of chloride ions in the solution increased and decreased regularly (Figure 2(a)). A similar pattern was observed when measuring iron ions present in solution. Additionally, it was observed that with increasing contact time, the solution turned from bright

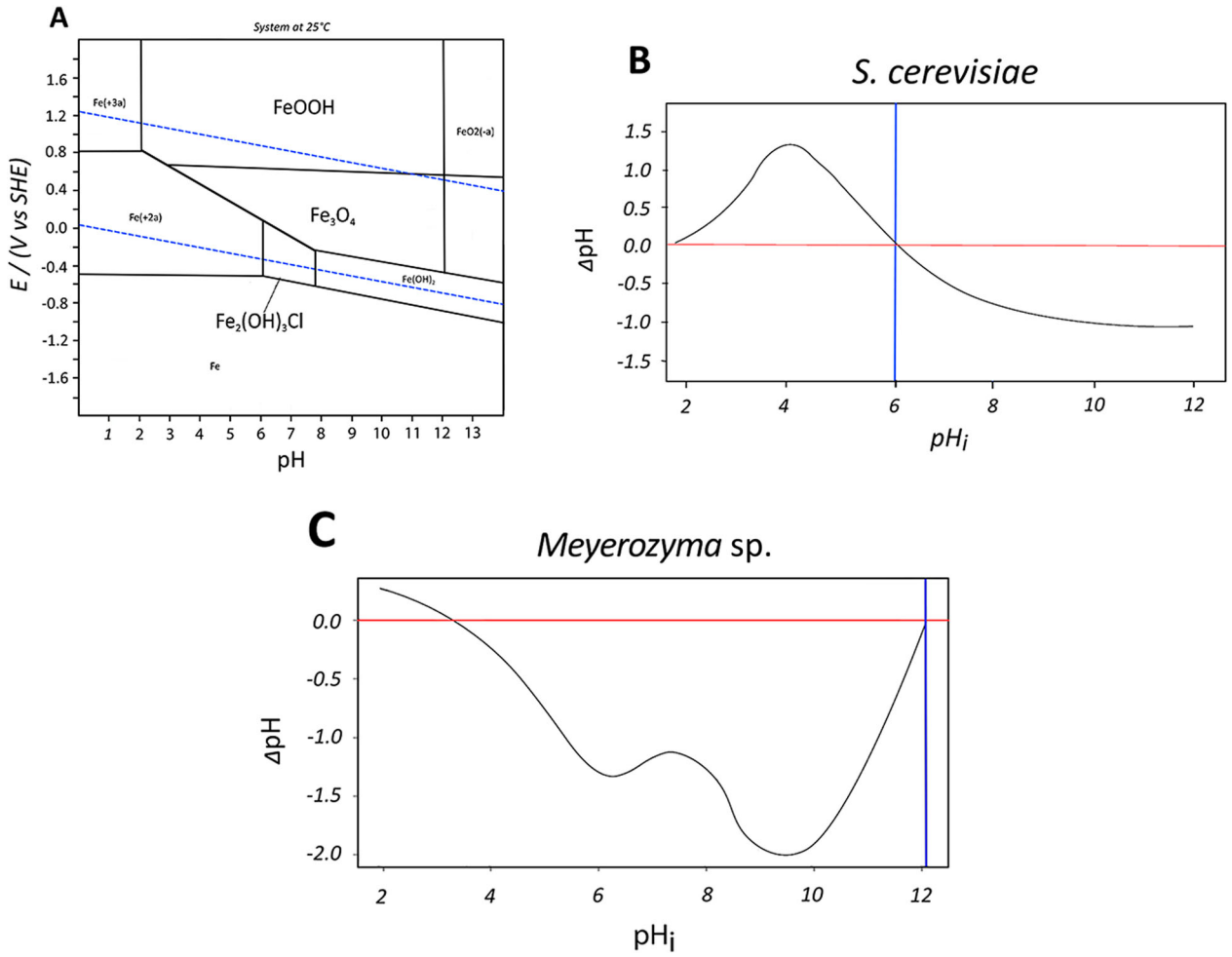

Figure 1. (a) E/pH diagram of Fe-H_2O-Cl^- Diagram was generated using the thermodynamic data published in Rémazeilles et al. 2009, (b) plot of pH_{pzc} for *S. cerevisiae*, and (c) for *Meyerozyma* sp. The pH_{pzc} value is calculated at the intersection of the red and blue lines.

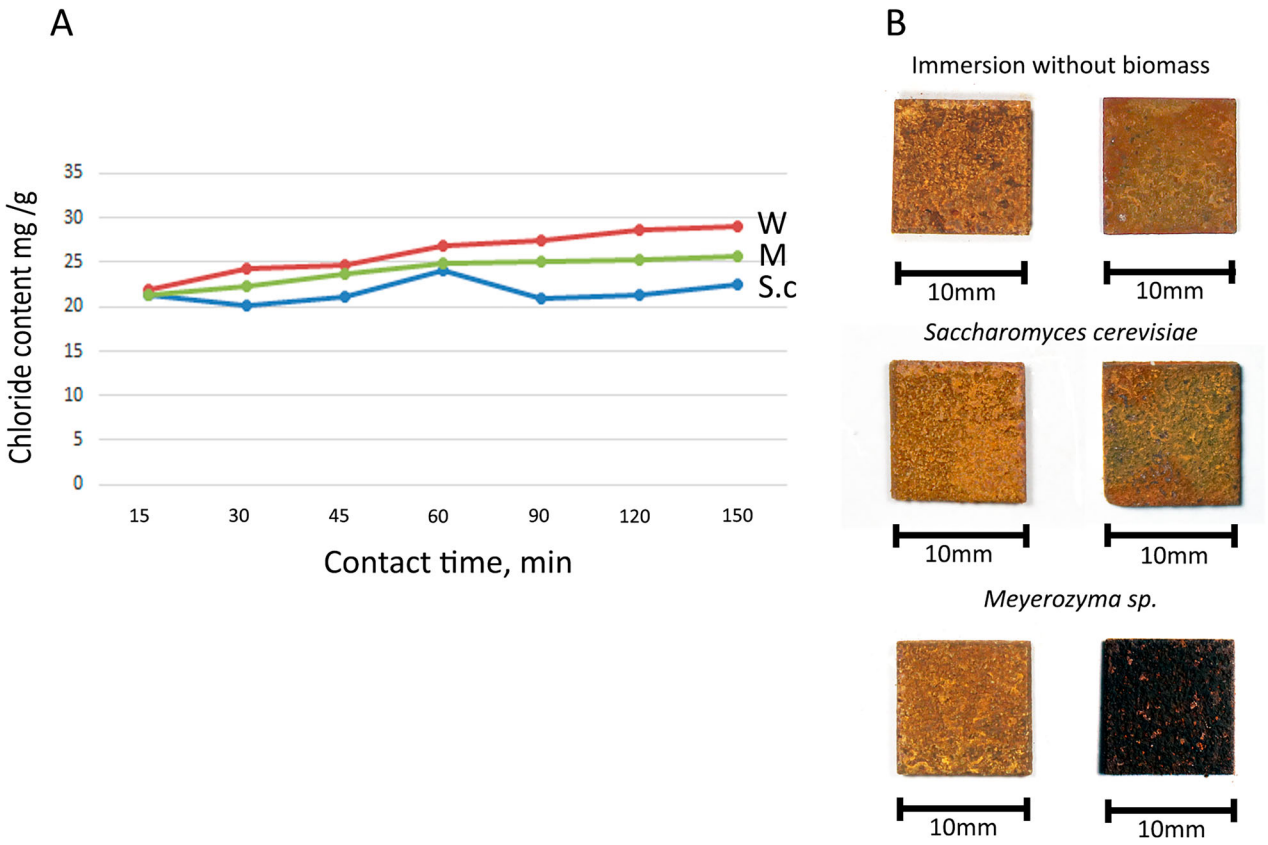

Figure 2. (a) Effect of contact time for biosorption effectiveness: w – immersion without biomass, M – with *Meyerozyma* sp., S.c – *S. cerevisiae*; (b) Surface aspect of the iron samples before and after treatment observed after 150 min of contact time.

orange to transparent. The surface aspect of the iron samples also changed. The initial dark orange corrosion layer (i.e. akaganeite) became less uniform, and the presence of a blue, green, yellow layer was observed (Figure 2(b)). These phases were identified as mixture of lepidocrocite, magnetite and akageneite by Raman spectroscopy (Figure 3).

When the same experiment was carried out with *Meyerozyma* sp. biomass, biosorption capacity was not altered as the contact time increased For the first 90 min, the chloride ion concentration increased and then some adsorption was observed, with an average of 0.2 mg/g (Figure 2(a)). The pH of the solution dropped from 7 to 4, as in the case of *S. cerevisiae*. The color of the solution also shifted during the experiment from vivid orange to translucent. The use of *Meyerozyma* sp. dry biomass also resulted in a change in the artificially-aged iron surface appearance (Figure 2(b)). In this case, the surface went from a dark orange corrosion product to a black uniform and slightly powdery layer identified as magnetite by Raman spectroscopy (Figure 3).

Biosorption Raman spectroscopy analysis

Before the experiment, Raman analysis of artificially-aged iron samples indicates that the main phase occurring on the surface is akageneite with typical vibrational bands identified at 140, 310 and 390 cm^{-1}, and additional weak peaks observed at 121, 205, 487, 537, 607, 720 and 910 cm^{-1} (Figure 3(a)). Peaks at 310 and 390 cm^{-1} are assigned to Fe– O vibration mode of Fe octahedrons present in its structure (Richmond et al. 2004). The third peak at 140 cm^{-1} is likely to correspond to Fe – Cl. Raman peaks observed at 535, 722 and 921 cm^{-1} could be assigned to Fe– OH asymmetric stretching (Szybowicz et al. 2015).

Artificially-aged iron coupons treated with *Meyerozyma* sp. showed a transformation of the corrosion products present on the surface from akageneite to magnetite (Figure 3(b)). An intense peak was noticed at 670 cm^{-1} as well as two weak peaks at 311 and 530 cm^{-1}, all indicating the presence of magnetite.

In comparison to *Meyerozyma* sp., artificially-aged iron samples exposed to *S. cerevisiae* dry biomass presented a less uniform surface appearance after treatment, and corrosion products such as akaganeite and lepidocrocite mixed with goethite were identified (Figure 3(c)). The mixture of lepidocrocite and goethite was characterized by the presence of intense peaks at 249, 299, 384 and 670 cm^{-1} and weak peaks at 485 and 527 cm^{-1} (Cambier, Verreault, and Frankel 2014).

SEM-EDX

To assess if changes occurring on the iron samples surfaces were related to interaction with the biosorbent, SEM-EDS was carried out on biomass of both yeast

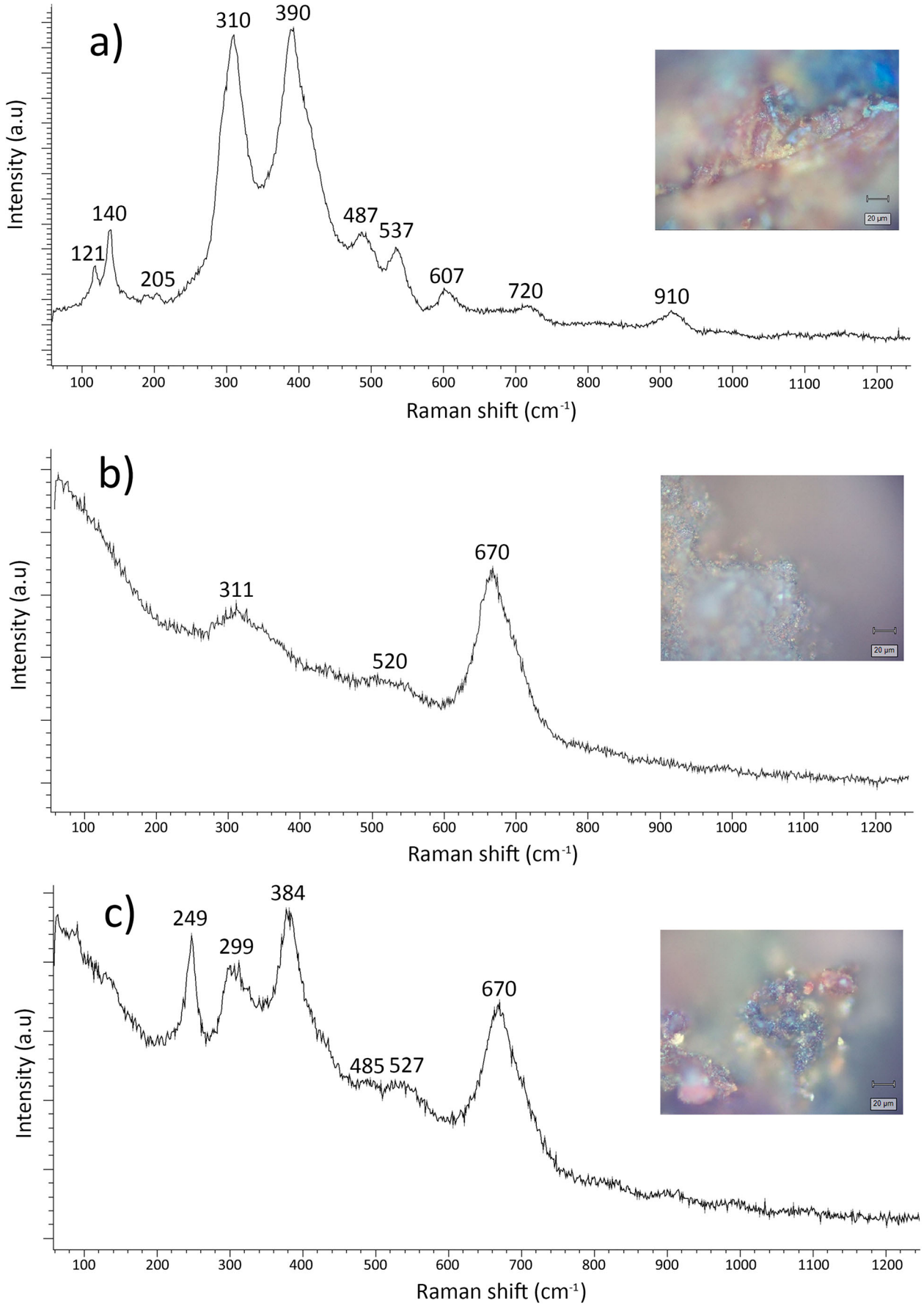

Figure 3. Raman spectra. (a) artificially-aged iron coupon before contact with biomass, (b) after exposure to dry biomass of *Meyerozyma* sp. (c) after exposure to dry biomass of *S. cerevisiae*. Instrumental settings: 785 nm, 3 mW, 7 s, 15 accumulations.

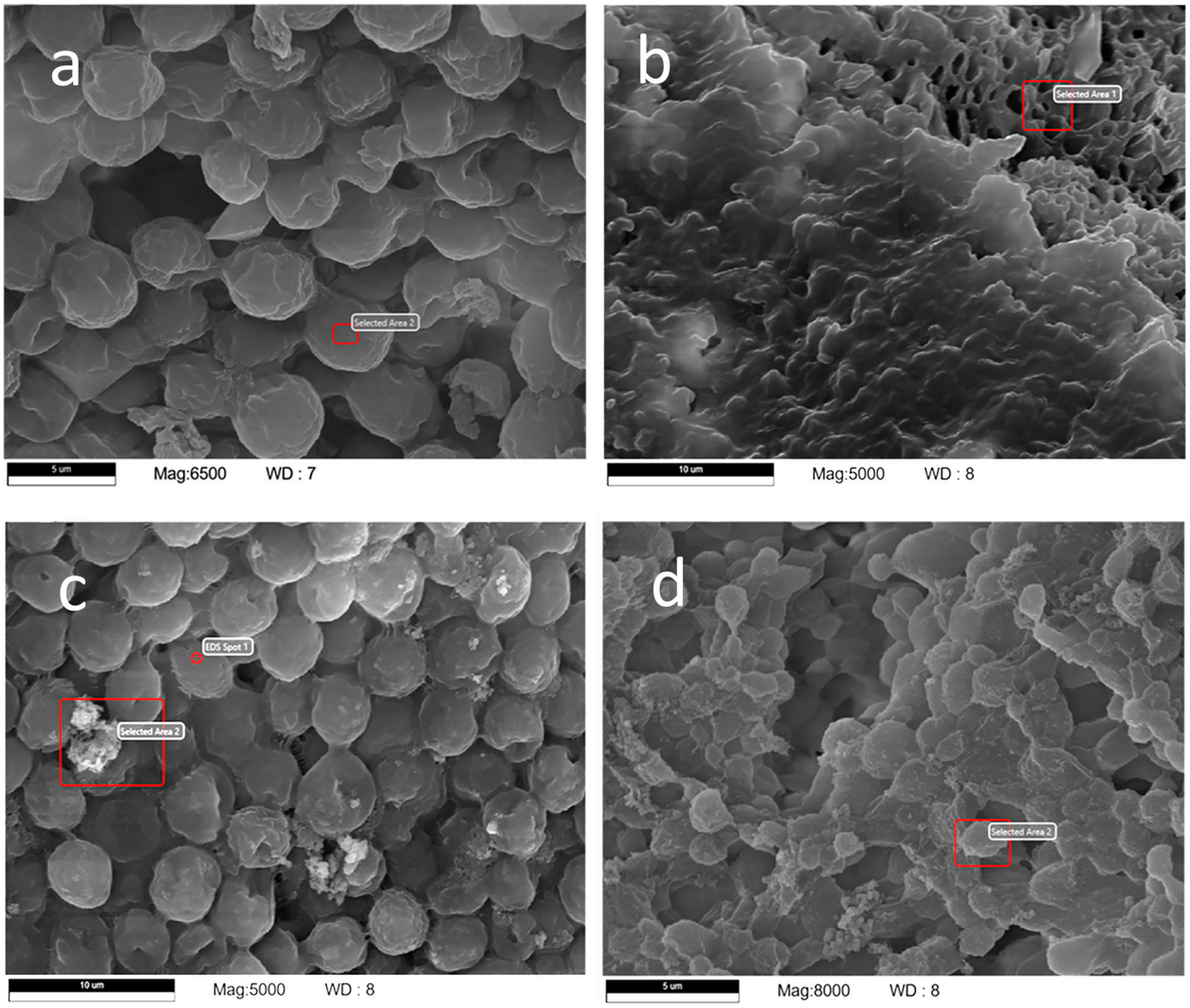

Figure 4. SEM images of dry biomass of (a) *S. cerevisiae* and (b) *Meyerozyma* sp. before biosorption; and of (c) *S. cerevisiae* (d) *Meyerozyma* sp. after biosorption. Areas outlined in red indicate the EDX analysis sites.

strains. During observation of *S. cerevisiae*, irregularity and roughness of the cell wall was clearly spotted on untreated dry biomass. In several areas cracks were visible on the cell wall (Figure 4(a)). This may be associated with the process of drying biomass at high temperature (Cutz et al. 2021).

The surface morphology of the cell wall changed after being in contact with artificially-aged iron samples. SEM images showed a smoother surface and a complete disappearance of cracks after the experiment (Figure 4(c)). EDS analysis confirmed the presence of chloride in both untreated and treated biomass. Additionally, in the sample treated with *S. cerevisiae* a new element – iron – was observed. Higher contents of this element were localized in the brighter spots (Figure 4(c)).

The same protocol was used to observe the *Meyerozyma* sp. cell wall. SEM images of fungal dry biomass revealed a porous and rough surface with many voids before the biosorption experiment (Figure 4(b)). After exposure to artificially-aged iron samples, *Meyerozyma* biomass showed distinct changes on the cell wall surface that became swollen and covered with bright small particles (Figure 4(d)). Changes in the elemental composition were recorded with EDS. Analysis after biosorption showed the presence of two additional elements, iron and chloride. Additionally, these results indicated that the biosorption of iron was almost five times higher than the biosorption of chloride.

FTIR

FTIR spectra of biomass of *S. cerevisiae* and *Meyeroyzma* sp. were recorded before and after the experiments to identify the functional groups potentially involved in the process of biosorption. FTIR spectra revealed highly complex molecular structures for both *Meyrozyma* sp. and *S. cerevisiae* strains (Table 1). After the biosorption experiment, for both fungi, shifts in wavenumbers and relative intensity were observed.

FTIR spectra of *S. cerevisiae* biomass revealed involvement of several functional groups such as hydroxyl groups – OH, amines – NH_2, amides $RCONH_2$, and alkyl chains – CH_2, – CH_3. Also, C = O, amide III and

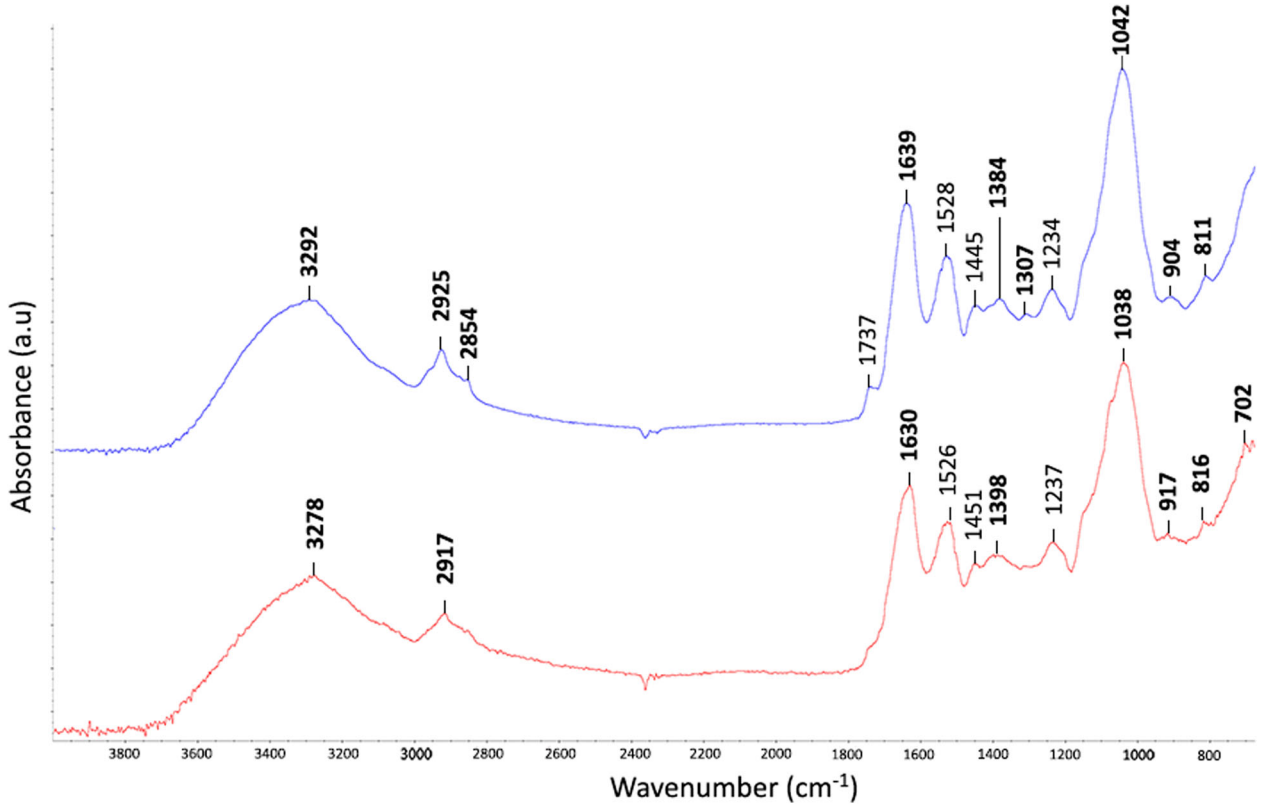

Figure 5. FTIR spectra of dry biomass of *S. cerevisiae* before biosorption (red) and after immersion with artificially-aged iron sample (blue). Shifts in wavenumbers or relative intensity are indicated in bold.

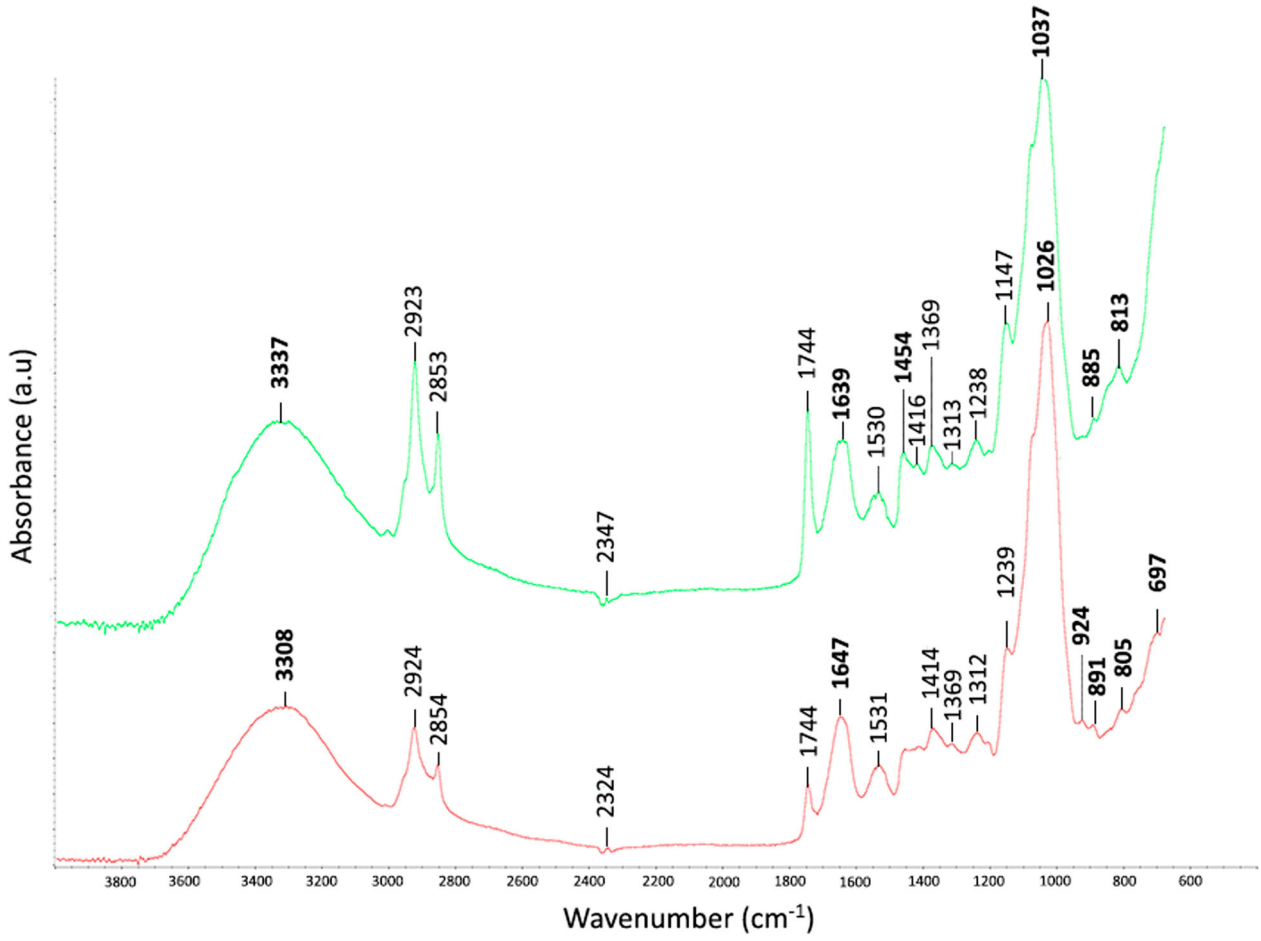

Figure 6. FTIR spectra of dry biomass of *Meyerozyma* sp. before biosorption (red) and after immersion with artificially-aged iron sample (green). Shifts in wavenumbers or relative intensity are indicated in bold.

Table 1. FTIR peak assignment for *S. cerevisiae* and *Meyerozyma* sp. before and after the biosorption experiment.

S. cerevisiae Wavenumbers (cm^{-1})		Meyerozyma sp. Wavenumbers (cm^{-1})		
Dry biomass	Exposed dry biomass	Dry biomass	Exposed dry biomass	Functional group assignment
3278	**3292**	**3308**	**3337**	**O–H and** amines N–H stretching vibration
2917	**2925**	2924	2923	CH_2, CH_3
–	2854	2854	2853	CH_2, CH_3
–	–	2342	2347	CO_2
–	1737	1744	1744	C=O
1630	**1639**	**1647**	**1639**	**Amide I**
1526	1528	1531	1530	Amide II
1451	1445	–	**1454**	CH_2
–	–	1414	1416	C–N
1398	**1384**	1369	1369	$C(CH_3)_2$ symmetric
–	**1307**	1312	1313	Amide III
1237	1234	1239	1238	ν(P=O) asymmetric
–	–	1148	1147	δ(COP), ν (CC), δ(COH)
1038	**1042**	**1026**	**1037**	νC–O of polysaccharides nucleic acids, polysaccharides skeleton –C–OH
917	**904**	**924**	–	Carbohydrates
–	–	**891**	**885**	glycosidic linkage
816	**811**	**805**	**813**	C – H bonds
702	–	**697**	–	C – C twisting

Note: Green color indicates bands with observed shifts of wavenumbers.

polysaccharide bands had changed relative intensity after the biosorption experiment (Figure 5).

The results obtained with *Meyerozyma* sp. biomass suggested that an ion exchange process could be associated with hydroxyl groups, primary and secondary amines, amides and polysaccharides, as indicated by the shift in wavenumbers after the experiment. Additionally, changes in relative intensity of C = O and amide II bands were observed, which implied that these functional groups may also play a role in the biosorption process (Figure 6).

XRF

XRF analysis was conducted to evaluate chloride removal from the artificially-aged iron samples. The highest extraction of chloride ions was recorded with *Meyerozyma* sp. (96% of biomass biosorption) followed by *S. cerevisiae* (78% of biomass biosorption) at a contact time of 90 minutes and biosorbent dosage of 0.02 g. A certain amount (74% biomass biosorption) of chloride ions was also removed by osmotic diffusion in water without biomass as sorbent.

Conclusion

Currently available methods for archeological iron stabilization present several disadvantages including efficiency and safety concerns for human health and environment. For these reasons it is necessary to search for new solutions that will be effective and more sustainable.

During preliminary tests presented in this article the potential of *Meyerozyma* sp. and *S. cerevisiae* for the removal of chloride ions from aqueous solution has been explored. Contact time experiments conducted on artificially-aged iron samples revealed promising feasibility to develop green stabilization treatments based on fungal biomass biosorption.

The results obtained with *S. cerevisie* (obtained as a waste product from beer production) showed the ability to passively bind chloride ions onto surface of fungal cell walls. The biggest increase in the biosorption efficiency was recorded after 90 min of exposure at pH 4 and biomass dosage 0.02 g. However, unexpected processes of adsorption and desorption were noticed after 150 min of contact time. A hypothesis regarding this phenomenon could be associated with impurities present in the initial biomass. In fact, SEM-EDX results confirmed the presence of chloride ions in untreated and treated biomass. One of the possible limitations observed with *S. cerevisiae* is the visual appearance of artificially-aged iron samples after biosorption that may not comply with the conservator aesthetics requirements for archaeological iron artefacts post-conservation.

The outcome obtained from the *Meyerozyma* sp. experiments shows two possible ways of using dry biomass for iron stabilization. SEM-EDX results confirmed the ability of *Meyerozyma* sp. to biosorb chloride and iron ions onto the cell walls. Secondly unexpected changes in appearance of the artificially-aged iron sample surfaces treated with *Meyerozyma* sp. suggested the conversion of reactive corrosion products into more stable compounds. In fact, Raman analysis showed a transformation of corrosion products from akageneite to magnetite. This phenomenon might be associated with an ion exchange process occurring between the iron sample and functional groups present on the fungal cell wall surface. Nevertheless, more research would be needed to fully understand the reaction that leads to this conversion of reactive corrosion products into more chemically stable compounds.

In comparison to traditional methods, the preliminary experiments with biomass biosorption on *Meyerozyma* sp. and *S. cerevisiae* present numerous advantages towards ethical environmental practices such as health and safety, environmental impact, and waste management. Additionally treatment with nonliving biomass showed good results regarding time of application. This outcome will lead to a reduction of water use during the desalination process while maintaining a high extraction rate. Nevertheless, the greatest achievement shown in this article is the absence of toxic materials used during the desalination process. Treatment based on dry biomass and water provides a safer formula, without concerns of human health and environmental pollution. These findings are promising

and provide a solid basis for future optimization in the creation of an efficient and sustainable conservation method for archaeological iron stabilization.

Acknowledgements

The Swiss Centre for Electronics and Microtechnology (CSEM) especially to Dr. O. Sereda and B. Gaëtan for SEM-EDS.

Disclosure statement

No potential conflict of interest was reported by the author(s).

Funding

HESSO is an associated partner in the framework of the GoGreen *Strategies to Conserve the Past and Preserve the Future of Cultural Heritage*, Horizon-RIA project 2022–2026 [grant number 101060768]. The participation is funded by the State Secretary for Education, Research and Innovation (SERI) [grant number 22-00121] as transitional measures program for Horizon 2021–2027.

References

Al-Maliky, E. A., H. A. Gzar, and M. G. Al-Azawy. 2021. "Determination of Point of Zero Charge (PZC) of Concrete Particles Adsorbents." *IOP Conference Series: Materials Science and Engineering* 1184: 012004. https://doi.org/10.1088/1757-899X/1184/1/012004.

Amorim, S. S., F. A. Dias Ruas, N. Rocha Barboza, V. G. de Oliveira Neves, V. A. Leão, and R. Guerra-Sá. 2018. "Manganese (Mn^{2+}) Tolerance and Biosorption by *Meyerozyma guilliermondii* and *Meyerozyma caribbica* Strain." *Journal of Environmental Chemical Engineering* 6 (4): 4538–4545. https://doi.org/10.1016/j.jece.2018.06.061.

Azoulay, I., E. Conforto, P. Refait, and C. Remazeilles. 2013. "Study of Ferrous Corrosion Products on Iron Archaeological Objects by Electron Backscattered Diffraction (EBSD)." *Applied Physics A* 110: 379–388. https://doi.org/10.1007/s00339-012-7174-1.

Cambier, S., D. Verreault, and G. S. Frankel. 2014. "Raman Investigation of Anodic Undermining of Coated Steel During Environmental Exposure." *Corrosion* 70 (12): 1219–1229. https://doi.org/10.5006/1358.

Comensoli, L., J. Maillard, M. Albini, F. Sandoz, P. Junier, and E. Joseph. 2017. "Use of Bacteria to Stabilize Archaeological Iron." *Applied and Environmental Microbiology* 83 (9): e03478-16. https://doi.org/10.1128/AEM.03478-16.

Cutz, L., U. Tiringer, H. Gilvari, D. Schott, A. Mol, and W. de Jong. 2021. "Microstructural Degradation During the Storage of Biomass Pellets." *Communications Materials* 2 (2): 1–12. https://doi.org/10.1038/s43246-020-00113-y.

Drews, M. J., N. G. González-Pereyra, P. Mardikian, and P. de Viviés. 2013. "The Application of Subcritical Fluids for the Stabilization of Marine Archaeological Iron." *Studies in Conservation* 58 (4): 314–325. https://doi.org/10.1179/2047058412Y.0000000079.

Glotch, T. D., and M. D. Kraft. 2008. "Thermal Transformations of Akaganeite and Lepidocrocite to Hematite: Assessment of Possible Precursors to Martian Crystalline Hematite." *Physics and Chemistry of Minerals* 35: 569–581. https://doi.org/10.1007/s00269-008-0249-z.

Hu, Y., Z. Zhu, J. Nielsen, and V. Siewers. 2019. "Engineering *Saccharomyces cerevisiae* Cells for Production of Fatty Acid-derived Biofuels and Chemicals." *Open Biology* 9 (5): 190049. https://doi.org/10.1098/rsob.190049.

Ivanova, T., M. Maier, A. Missarova, C. Ziegler-Birling, M. Dam, M. Gomar-Alba, L. B. Carey, and M. Mendoza. 2020. "Budding Yeast Complete DNA Synthesis After Chromosome Segregation Begins." *Nature Communications* 11: 2267. https://doi.org/10.1038/s41467-020-16100-3.

Kampasakali, E., T. Fardi, E. Pavlidou, and D. Christofilios. 2021. "Towards Sustainable Museum Conservation Practices: A Study on the Surface Cleaning of Contemporary Art and Design Objects with the Use of Biodegradable Agents." *Heritage* 4 (3): 2023–2043. https://doi.org/10.3390/heritage4030115.

Kergourlay, F., S. Réguer, D. Neff, F. Foy, F.-E. Picca, M. Saheb, S. Hustache, F. Mirambet, and P. Dillmann. 2018. "Stabilization Treatment of Cultural Heritage Artefacts: *In Situ* Monitoring of Marine Iron Objects Dechlorinated in Alkali Solution." *Corrosion Science* 132: 21–34. https://doi.org/10.1016/j.corsci.2017.12.028.

Lasch, P., and D. Naumann. 2000. "Infrared Spectroscopy in Microbiology." In *Encyclopedia of Analytical Chemistry*, edited by R. A. Meyers, 102–131. London: Wiley.

Michalak, I., K. Chojnacka, and A. Witek-Krowiak. 2013. "State of the Art for the Biosorption Process—a Review." *Applied Biochemistry and Biotechnology* 170 (6): 1389–1416. https://doi.org/10.1007/s12010-013-0269-0.

Navarro-Arias, M. J., M. J. Hernández-Chávez, L. C. García-Carnero, D. G. Amezcua-Hernández, N. E. Lozoya-Pérez, E. Estrada-Mata, I. Martínez-Duncker, B. Franco, and H. M. Mora-Montes. 2019. "Differential Recognition of *Candida tropicalis*, *Candida guilliermondii*, *Candida krusei*, and *Candida auris* by Human Innate Immune Cells." *Infection and Drug Resistance* 12: 783–794. https://doi.org/10.2147/IDR.S197531.

Paulissen, S. M., C. A. Hunt, B. C. Seitz, C. J. Slubowski, Y. Yu, X. Mucelli, D. Truong, et al. 2020. "Noncanonical Hippo Pathway Regulates Spindle Disassembly and Cytokinesis During Meiosis in *Saccharomyces cerevisiae*." *Genetics* 216 (2): 447–462. https://doi.org/10.1534/genetics.120.303584.

Reguer, S., F. Mirambet, E. Dooryhee, J.-L. Hodeau, P. Dillmann, and P. Lagarde. 2009. "Structural Evidence for the Desalination of Akaganeite in the Preservation of Iron Archaeological Objects, Using Synchrotron X-ray Powder Diffraction and Absorption Spectroscopy." *Corrosion Science* 51 (12): 2795–2802. https://doi.org/10.1016/j.corsci.2009.07.012.

Rémazeilles, C., D. Neff, F. Kergourlay, E. Foy, E. Conforto, E. Guilminot, S. Reguer, Ph. Refait, and Ph. Dillmann. 2009. "Mechanisms of Long-Term Anaerobic Corrosion of Iron Archaeological Artefacts in Seawater." *Corrosion Science* 51 (12): 2932–2941. https://doi.org/10.1016/j.corsci.2009.08.022.

Richmond, W. R., J. G. Hockridge, M. Loan, and G. M. Parkinson. 2004. "A New Iron Oxyhydroxide Phase: The Molybdate-Substituted Analogue of Akaganéite." *Chemistry of Materials* 16 (17): 3203–3205. https://doi.org/10.1021/cm049261o.

Rimmer, M., D. Watkinson, and Q. Wang. 2012. "The Efficiency of Chloride Extraction from Archaeological Iron Objects Using Deoxygenated Alkaline Solutions." *Studies in Conservation* 57: 29–41. https://doi.org/10.1179/2047058411Y.0000000005.

Selwyn, L. 2004. "Overview of Archaeological Iron: The Corrosion Problem, Key Factors Affecting Treatment,

and Gaps in Current Knowledge." In *Metal 04: Proceedings of the International Conference on Metals Conservation*, 294–306. Canberra: National Museums of Australia.

Simon, H. J., G. Cibin, C. Reinhard, Y. Liu, E. Schofield, and I. C. Freestone. 2019. "Influence of Microstructure on the Corrosion of Archaeological Iron Observed Using 3D Synchrotron Micro-Tomography." *Corrosion Science* 159: 108132. https://doi.org/10.1016/j.corsci.2019.108132.

Stookey, L. L. 1970. "Ferrozine – A New Spectrophotometric Reagent for Iron." *Analytical Chemistry* 42 (7): 779–781. https://doi.org/10.1021/ac60289a016.

Szybowicz, M., M. Koralewski, J. Karoń, and M. Melnikova. 2015. "Micro-Raman Spectroscopy of Natural and Synthetic Ferritins and Their Mimetics." *Acta Physica Polonica A* 127 (2): 534–536. https://doi.org/10.12693/APhysPolA.127.534.

Turgoose, S. 1993. "Structure, Composition and Deterioration of Unearthed Iron Objects." In *Current Problems in the Conservation of Metal Antiquities*, edited by A. Shigeo, 35–52. Tokyo: Tokyo National Research Institute of Cultural Properties.

Vietti, A., E. Angelini, S. Grassini, and N. Donato. 2022. "Raman Spectroscopic Characterization of Corrosion Products of Archaeological Iron." *Journal of Physics: Conference Series* 2204: 012066. https://doi.org/10.1088/1742-6596/2204/1/012066.

Watkinson, D. 2010. "Measuring Effectiveness of Washing Methods for Corrosion Control of Archaeological Iron: Problems and Challenges." *Corrosion Engineering, Science and Technology* 45: 400–406. https://doi.org/10.1179/147842210X12754747500801.